AD-A119505

BEST AVAILABLE COPY

UNCLASSIFIED

SECURITY CLASSIFICATION OF THIS PAGE (When Data Entered)

REPORT DOCUMENTATION PAGE		READ INSTRUCTIONS BEFORE COMPLETING FORM
1. REPORT NUMBER NSWC TR 81-456	2. GOVT ACCESSION NO. AD-A119505	3. RECIPIENT'S CATALOG NUMBER Final
4. TITLE (and Subtitle) A MATHEMATICAL DESCRIPTION OF THE LOW-ALTITUDE SATELLITE MISSION PLANNING TOOL (LAMP)		5. TYPE OF REPORT & PERIOD COVERED 6. PERFORMING ORG. REPORT NUMBER
7. AUTHOR(s) A. D. Parks		8. CONTRACT OR GRANT NUMBER(s) 63701B; 2K12CSR24
9. PERFORMING ORGANIZATION NAME AND ADDRESS Naval Surface Weapons Center (K13) Dahlgren, Virginia 22448		10. PROGRAM ELEMENT, PROJECT, TASK AREA & WORK UNIT NUMBERS
11. CONTROLLING OFFICE NAME AND ADDRESS Defense Mapping Agency Washington, DC 20305		12. REPORT DATE January 1982 13. NUMBER OF PAGES 39
14. MONITORING AGENCY NAME & ADDRESS(if different from Controlling Office)		15. SECURITY CLASS. (of this report) UNCLASSIFIED 15a. DECLASSIFICATION/DOWNGRADING SCHEDULE

16. DISTRIBUTION STATEMENT (of this Report)

Approved for public release; distribution unlimited.

17. DISTRIBUTION STATEMENT (of the abstract entered in Block 20, if different from Report)

DTIC
ELECTE
SEP 22 1982
D
H

18. SUPPLEMENTARY NOTES

19. KEY WORDS (Continue on reverse side if necessary and identify by block number)

Low-Altitude Mission Planning (LAMP)
Keplerian orbit parameters; predictions of
Satellites, low altitude
Lagrange Planetary equations

20. ABSTRACT (Continue on reverse side if necessary and identify by block number)

The Low-Altitude Mission Planning tool is capable of providing accurate long-term (~90 day) predictions of key Keplerian orbit parameters and related quantities for one or two low-altitude satellites. Analytically modeled averaged variational equations are used to represent the effects of the geopotential oblateness upon satellite motion. Satellite drag perturbations are taken into account using a hybrid drag decay model which accounts for atmospheric oblateness and diurnal density variation. Adjustments to orbital parameters due to thrusting are modeled using ana-

(see back)

DD FORM 1 JAN 73 1473 EDITION OF 1 NOV 65 IS OBSOLETE
S/N 0102-LF-014-6601

UNCLASSIFIED

SECURITY CLASSIFICATION OF THIS PAGE (When Data Entered)

(20)

lytical results obtained from the Lagrange Planetary equations when impulsive thrusting is assumed. Propellant mass expenditures can also be obtained. This planning tool has application in the following areas:

(1) Operational interruption prediction;
(2) Propellant depletion rate studies;
(3) Operational flight strategy development;
(4) Orbit adjust impact assessment, and
(5) General mission planning.

FOREWORD

This report was prepared by A. D. Parks to describe a mission planning software tool which is anticipated to have certain utility in the support of several Defense Mapping Agency satellite programs. This report was reviewed and approved by R. J. Anderle and R. W. Hill.

Released by:

C. A. Fisher

C. A. FISHER, Head
Strategic Systems Department

Accession For
NTIS GRA&I ☑
DTIC TAB ☐
Unannounced ☐
Justification

By
Distribution/
Availability Codes
Dist | Avail and/or Special
A

DTIC COPY INSPECTED 8

CONTENTS

Section		Page
1.	INTRODUCTION	1
2.	EPHEMERIS GENERATION	1
	2.1 Force Model	1
	2.2 Mean Element Prediction	1
	2.3 Osculating Element Prediction	3
	2.4 Averaged Variational Equations Due to J_2, J_3, and J_4	4
	2.5 Semianalytic Atmospheric Drag Decay Rates	6
	2.6 First Order Short Periodic Variations	9
	2.7 Instantaneous Orbit Parameter Changes Due to Impulsive Thrusting	11
3.	INITIALIZATION	13
	3.1 Initial Condition Transformations	13
	3.2 Brouwer-Lyddane Transformation Theory	13
4.	AUXILIARY COMPUTATIONS	18
	4.1 Initialization and OEP Support Computations	18
	4.2 Drag Decay Rate Support Computations	20
	4.3 Model Atmosphere Peripheral Support Computations	22
	4.4 User Support Computations	24
5.	SOFTWARE DESIGN CONSIDERATIONS	25
	5.1 Basic Requirements	25
	5.2 Basic Computational Flow	26

TABLES

Table		Page
5-1	Operational Options	27
5-2	Output Options	28
5-3	Input Data Definitions	29

FIGURE

Figure		Page
5-1	LAMP Computational Overview	30

1. INTRODUCTION

The Low Altitude satellite Mission Planner (LAMP) is an analytic orbit planning software tool which can be used to estimate the decay history/lifetime and to generate orbital ephemerides for one or two close-Earth satellites ($.01 \lesssim e \lesssim .10$) perturbed by atmospheric drag and by Earth oblateness due to the zonal harmonics J_2, J_3, and J_4. LAMP is capable of providing rapid and accurate long term ($\sim$ 90 day) predictions of key Keplerian orbit parameters (a, e, i, Ω, ω) and related quantities (e.g. perigee and apogee altitudes; drag decay rates; period; theoretical atmospheric density profiles and scale heights; orbital phase angles) without resorting to time consuming numerical integration schemes. It can also use input orbit adjust designs to compute the associated changes to orbit parameters and make post orbit adjust predictions. A multiple orbit adjust capability exists so that propellant and thruster lifetime estimates can be made. It is thus likely that LAMP can be successfully applied to the analysis of problems in the following areas:

(i) general mission planning;
(ii) flight strategy development;
(iii) orbit adjust impact assessment;
(iv) propellant depletion rate studies; and
(v) operational interruption prediction.

The following sections discuss in detail both the mathematical and the processing methodologies employed within LAMP. Included in this discussion are descriptions of the ephemeris generation capabilities; the drag decay rate theory used by LAMP; the effect of impulsive thrusting upon orbit parameters; LAMP initialization techniques; auxiliary computations required to support processing; and input/output options.

2. EPHEMERIS GENERATION

2.1 Force Model

For most close-Earth, low altitude artificial satellites with small eccentricities, the only perturbations which need be considered are those produced by the second through the fourth zonal harmonics of the geopotential function, i.e. the J_2, J_3, and J_4 terms, and atmospheric drag deceleration. The perturbations due to other forces, e.g. higher order geopotential perturbations, solar radiation pressure, luni-solar effects, etc., are generally much smaller than the effects induced by the basic uncertainties in the knowledge of the atmospheric density and satellite ballistic coefficient. Consequently, the geopotential oblateness perturbations due to J_2, J_3, and J_4 and the atmospheric drag perturbation are the only continuous forces modeled in LAMP. The effect of perturbations due to periodic impulsive thrusting is also modeled in LAMP.

2.2 Mean Element Prediction

The mean orbital element prediction capability (MEP) is the foundation for all significant computations performed by LAMP. MEP is capable of generating predicted mean Keplerian orbital elements (a_m, e_m, i_m, Ω_m, ω_m, M_m) from initial conditions at time intervals Δt for

either short periods of time (i.e. hours or days) or long periods of time (i.e. weeks or months). When MEP is operating in the short term prediction mode (STP), Δt is taken to be a fixed time interval, whereas when MEP is operating in the long term prediction mode (LTP), Δt is taken to be the approximate current nodal period τ.

The algorithm used to generate predicted mean Keplerian elements at time t_i, i.e. the MEP algorithm, is:

$$\left.\begin{aligned}
a_m(t_i) &= a_m(t_{i-1}) + \left[\frac{\Delta a_D(t_{i-1})}{\tau_{i-1}}\right] \Delta t + \Delta a_{OA}(t_{i-1})\, \delta_{t_{OA},\Delta t} \,, \\
e_m(t_i) &= e_m(t_{i-1}) + \left\langle \dot{e}_G(t_{i-1}) \right\rangle \Delta t + \left[\frac{\Delta e_D(t_{i-1})}{\tau_{i-1}}\right] \Delta t + \Delta e_{OA}(t_{i-1})\, \delta_{t_{OA},\Delta t} \,, \\
i_m(t_i) &= i_m(t_{i-1}) + \left\langle i_G(t_{i-1}) \right\rangle \Delta t + \Delta i_{OA}(t_{i-1})\, \delta_{t_{OA},\Delta t} \,, \\
\Omega_m(t_i) &= \Omega_m(t_{i-1}) + \left\langle \dot{\Omega}_G(t_{i-1}) \right\rangle \Delta t + \Delta \Omega_{OA}(t_{i-1})\, \delta_{t_{OA},\Delta t} \,, \\
\omega_m(t_i) &= \omega_m(t_{i-1}) + \left\langle \dot{\omega}_G(t_{i-1}) \right\rangle \Delta t + \Delta \omega_{OA}(t_{i-1})\, \delta_{t_{OA},\Delta t} \,, \\
M_m(t_i) &= M_m(t_{i-1}) + \left\langle \dot{M}_G(t_{i-1}) \right\rangle \Delta t + \Delta M_{OA}(t_{i-1})\, \delta_{t_{OA},\Delta t} \,,
\end{aligned}\right\} \tag{2.1}$$

and

$$\tau_i = \tau_{i-1} + \frac{3}{2} \left[\frac{\tau_{i-1}}{a_m(t_i)}\right] \left[\frac{\Delta a_D(t_i)}{\tau_{i-1}}\right] \Delta t + \Delta \tau_{OA}(t_{i-1})\, \delta_{t_{OA},\Delta t} \,,$$

where $t_i \epsilon \left[t_O, t_E\right]$, t_E is the end time for the prediction interval, and

$$\Delta t = \begin{cases} t_i - t_{i-1} & \text{for the STP mode} \\ \tau_{i-1} & \text{for the LTP mode.} \end{cases} \tag{2.2}$$

In equations (2.1) the quantities $\Delta X_D(t_{i-1})$ are the changes in the X_m orbital elements over one orbital revolution due to drag deceleration evaluated in terms of the mean orbital elements at time t_{i-1}; $\langle \dot{X}_G(t_{i-1}) \rangle$ are the rates of change of the X_m orbital elements due to J_2, J_3, and J_4 averaged with respect to mean anomaly and evaluated in terms of the mean orbital elements at time t_{i-1}; and ΔX_{OA} are the changes in the X_m orbital elements and nodal period due to impulsive thrusting and evaluated in terms of the mean orbital elements at t_{i-1}. The $\delta_{t_{OA},\Delta t}$ is a

Kronecker delta defined by:

$$\delta_{t_{OA},\,\Delta t} = \begin{cases} 1 \ , & \text{for } t_{i-1} < t_{OA} \leqslant t_i \\ 0 \ , & \text{otherwise} \ , \end{cases} \tag{2.3}$$

where t_{OA} is the time of the impulsive thrust. The quantities ΔX_D, ΔX_{OA}, and $\langle \dot{X}_G \rangle$ are discussed further in the following sections.

2.3 Osculating Element Prediction

The osculating element prediction capability (OEP) is generally used in conjunction with the MEP capability in the STP mode to generate predicted sets of osculating Keplerian orbital elements (a_{osc}, e_{osc}, i_{osc}, Ω_{osc}, ω_{osc}, M_{osc}) or Cartesian components at fixed time intervals Δt. The algorithm used to generate the osculating Keplerian elements at time t_i, i.e. the OEP algorithm, is:

$$\left.\begin{aligned} a_{osc}(t_i) &= a_m(t_i) + a_{sp}(t_i) \ , \\ e_{osc}(t_i) &= e_m(t_i) + e_{sp}(t_i) \ , \\ i_{osc}(t_i) &= i_m(t_i) + i_{sp}(t_i) \ , \\ \Omega_{osc}(t_i) &= \Omega_m(t_i) + \Omega_{sp}(t_i) \ , \\ \omega_{osc}(t_i) &= \omega_m(t_i) + \omega_{sp}(t_i) \ , \\ \text{and} \quad & \\ M_{osc}(t_i) &= M_m(t_i) + M_{sp}(t_i) \ , \end{aligned}\right\} \tag{2.4}$$

where (a_m, e_m, i_m, Ω_m, ω_m, M_m) are the mean Keplerian orbital elements at time t_i computed using the MEP algorithm of equations (2.1), and (a_{sp}, e_{sp}, i_{sp}, Ω_{sp}, ω_{sp}, M_{sp}) are the first order short periodic variations of the Keplerian element set evaluated using the mean Keplerian set at time t_i. These short periodic variations are discussed further in the following sections.

2.4 Averaged Variational Equations Due to J_2, J_3, and J_4

The averaged motion of a low altitude, close-Earth satellite resulting only from perturbations due to the second through the fourth zonal harmonic terms of the geopotential function, i.e. the $\langle \dot{X}_G \rangle$ factors of equations (2.1) are computed from the following expressions[1]:

$$\langle \dot{a}_G \rangle = 0 ,$$

$$\langle \dot{e}_G \rangle = -\frac{3}{32} nJ_2^2 \left(\frac{R}{p}\right)^4 \sin^2 i \,(14 - 15 \sin^2 i)\, e\,(1-e^2) \sin 2\omega - \frac{3}{8} nJ_3 \left(\frac{R}{p}\right)^3$$

$$\times \sin i \,(4-5 \sin^2 i)\,(1-e^2) \cos \omega - \frac{15}{32} nJ_4 \left(\frac{R}{p}\right)^4 \sin^2 i \,(6-7 \sin^2 i)\, e$$

$$\times (1-e^2) \sin 2\omega ,$$

$$\langle \dot{i}_G \rangle = \frac{3}{64} nJ_2^2 \left(\frac{R}{p}\right)^4 \sin 2i \,(14-15 \sin^2 i)\, e^2 \sin 2\omega + \frac{3}{8} nJ_3 \left(\frac{R}{p}\right)^3 \cos i \,(4-5 \sin^2 i)$$

$$\times e \cos \omega + \frac{15}{64} nJ_4 \left(\frac{R}{p}\right)^4 \sin 2i \,(6-7 \sin^2 i)\, e^2 \sin 2\omega ,$$

$$\langle \dot{\Omega}_G \rangle = -\frac{3}{2} nJ_2 \left(\frac{R}{p}\right)^2 \cos i - \frac{3}{2} nJ_2^2 \left(\frac{R}{p}\right)^4 \cos i \left[\frac{9}{4} + \frac{3}{2}\sqrt{1-e^2}\right.$$

$$\left. - \sin^2 i \left(\frac{5}{2} + \frac{9}{4}\sqrt{1-e^2}\right) + \frac{e^2}{4}\left(1 + \frac{5}{4}\sin^2 i\right) + \frac{e^2}{8}(7-15 \sin^2 i) \cos 2\omega\right]$$

$$- \frac{3}{8} nJ_3 \left(\frac{R}{p}\right)^3 (15 \sin^2 i - 4)\, e \cot i \sin \omega + \frac{15}{16} nJ_4 \left(\frac{R}{p}\right)^4 \cos i$$

$$\times \left[\left(4-7 \sin^2 i\right)\left(1 + \frac{3}{2} e^2\right) - (3-7 \sin^2 i)\, e^2 \cos 2\omega\right] ,$$

$$\langle \dot{\omega}_G \rangle = \frac{3}{4} nJ_2 \left(\frac{R}{p}\right)^2 (4-5 \sin^2 i) + \frac{3}{16} nJ_2^2 \left(\frac{R}{p}\right)^4 \left\{48-103 \sin^2 i\right.$$

$$+ \frac{215}{4} \sin^4 i + \left(7 - \frac{9}{2} \sin^2 i - \frac{45}{8} \sin^4 i\right) e^2$$

[1] Liu, J. J. F. and Alford, R. L., "Semianalytic Theory for a Close-Earth Satellite," *AIAA Journal of Guidance and Control,* Vol. 3, July-August 1980, pp. 304-311.

$$
\left.
\begin{aligned}
&+ 6\left(1 - \frac{3}{2}\sin^2 i\right)(4 - 5\sin^2 i)\sqrt{1-e^2} - \frac{1}{4}\left[2\,(14\right. \\
&\left. - 15\sin^2 i)\sin^2 i - (28 - 158\sin^2 i + 135\sin^4 i)\,e^2\right]\cos 2\omega\Big\} \\
&+ \frac{3}{8}\,nJ_3\left(\frac{R}{p}\right)^3\left[(4 - 5\sin^2 i)\,\frac{\sin^2 i - e^2\cos^2 i}{e\sin i} + 2\sin i\,(13\right. \\
&\left. - 15\sin^2 i)\,e\right]\sin\omega - \frac{15}{32}\,nJ_4\left(\frac{R}{p}\right)^4\Big\{16 - 62\sin^2 i \\
&+ 49\sin^4 i + \frac{3}{4}\,(24 - 84\sin^2 i + 63\sin^4 i)\,e^2 + \Big[\sin^2 i\,(6 \\
&- 7\sin^2 i) - \frac{1}{2}\,(12 - 70\sin^2 i + 63\sin^4 i)\,e^2\Big]\cos 2\omega\Big\},
\end{aligned}
\right\} \quad (2.5)
$$

and

$$
\begin{aligned}
\langle \dot{M}_G \rangle = {} & n\left[1 + \frac{3}{2}J_2\left(\frac{R}{p}\right)^2\left(1 - \frac{3}{2}\sin^2 i\right)\sqrt{1-e^2}\right] \\
& + \frac{3}{2}\,nJ_2^2\left(\frac{R}{p}\right)^4\Big\{\left(1 - \frac{3}{2}\sin^2 i\right)^2(1 - e^2) + \Big[\frac{5}{4}\Big(1 \\
& - \frac{5}{2}\sin^2 i + \frac{13}{8}\sin^4 i\Big) + \frac{5}{8}\left(1 - \sin^2 i - \frac{5}{8}\sin^4 i\right)e^2 \\
& + \frac{1}{16}\sin^2 i\,(14 - 15\sin^2 i)\left(1 - \frac{5}{2}e^2\right)\cos 2\omega\Big]\sqrt{1-e^2}\Big\} \\
& + \frac{3}{8}\,nJ_2^2\left(\frac{R}{p}\right)^4\frac{1}{\sqrt{1-e^2}}\Big\{3\Big[3 - \frac{15}{2}\sin^2 i + \frac{47}{8}\sin^4 i \\
& + \left(\frac{3}{2} - 5\sin^2 i + \frac{117}{16}\sin^4 i\right)e^2 - \frac{1}{8}\Big(1 + 5\sin^2 i \\
& - \frac{101}{8}\sin^4 i\Big)e^4\Big] + \frac{e^2}{8}\sin^2 i\Big[70 - 123\sin^2 i + (56
\end{aligned}
$$

$$- 66 \sin^2 i) e^2\Big] \cos 2\omega + \frac{27}{128} e^4 \sin^4 \cos 4\omega\Big\} - \frac{3}{8} nJ_3 \left(\frac{R}{p}\right)^3 \sin i$$

$$\times (4 - 5 \sin^2 i) \frac{1 - 4e^2}{e} \sqrt{1 - e^2} \sin \omega - \frac{45}{128} nJ_4 \left(\frac{R}{p}\right)^4 (8$$

$$- 40 \sin^2 i + 35 \sin^4 i) e^2 \sqrt{1 - e^2} + \frac{15}{64} nJ_4 \left(\frac{R}{p}\right)^4 \sin^2 i (6$$

$$- 7 \sin^2 i) (2 - 5e^2) \sqrt{1 - e^2} \cos 2\omega \quad ,$$

where R is the equatorial radius of the Earth, n is the mea otion given by

$$n = \left(\frac{\mu}{a^3}\right)^{1/2} \quad , \tag{2.6}$$

μ is the Earth's gravitational constant, and

$$p = a (1 - e^2) \; . \tag{2.7}$$

Note that when computing the $\langle \dot{X}_G \rangle$ in equations (2.2), mean Keplerian elements should be used in the right hand sides of equations (2.5).

2.5 Semianalytic Atmospheric Drag Decay Rates

For close-Earth satellites the principal drag effects are perturbations in a and e. The remaining effects are small and for computational efficiency have been ignored in equations (2.1). The changes in a_m and e_m per orbital revolution due to drag deceleration by an oblate atmosphere with diurnal density variation are given by:[2]

$$\Delta a_D = - 2\pi \, \delta \, \rho_o \, g a^2 \exp\left[-\beta a e - c \cos 2\omega\right] \cdot \Big\{ I_0 + 2eI_1 + FA\Big[I_1$$

$$+ \frac{1}{2} e (I_0 + 3I_2)\Big] + c \Big\{ I_2 + 2eI_3 + \frac{1}{2} FA\Big[I_1 + I_3 + \frac{1}{2} e\Big(I_0$$

$$+ 2I_2 + 5I_4\Big)\Big]\Big\} \cos 2\omega - \frac{1}{2} cFB \Big\{ I_1 - I_3 + \frac{1}{2} e\Big(I_0 + 4I_2$$

[2] Santora, F. A., "Satellite Drag Perturbations in an Oblate Atmosphere With Day-To-Night Density Variation," AIAA Paper 74-839, AIAA Mechanics and Control of Flight Conference, Anaheim, California, August 1974.

$$- 5I_4)\Big\} \sin 2\omega + \frac{1}{4} c^2 \left\{ I_0 + 2eI_1 + FA\left[I_1 + \frac{1}{2} e\ (I_0 + 3I_2)\right]\right\}$$

$$+ \frac{1}{4} c^2 \left\{ I_4 - e\ (I_3 - 3I_5) + \frac{1}{2} FA\left[I_3 + I_5 - \frac{1}{2} e\ (I_2 - 2I_4 - 7I_6)\right]\right\}$$

$$\times \cos 4\omega - \frac{1}{8} c^2\ FB \left\{ I_3 - I_5 + \frac{1}{2} e\ (I_2 - 8I_4 + 7I_6)\right\} \sin 4\omega\Big\}, \tag{2.8}$$

and

$$\Delta e_D = \frac{\Delta(ae)_D - e\Delta a_D}{a} \quad , \tag{2.9}$$

where

$$\Delta(ae)_D = - 2\pi\delta\rho_o ga^2 \exp\left[- \beta ae - c \cos 2\omega\right] \cdot \Big\{ I_1 + \frac{1}{2} e\ (3I_0 + I_2)$$

$$+ \frac{1}{2} FA \left[I_0 + I_2 + e\ (3I_1 + I_3)\right] + \frac{1}{2} c \left\{ I_1 + I_3 - \frac{1}{2} e\ (I_0$$

$$- 6I_2 - 3I_4) + \frac{1}{2} FA\left[I_0 + 2I_2 + I_4 + e\ (I_1 + 2I_3 + I_5)\right]\right\}$$

$$\times \cos 2\omega - \frac{1}{4} cFB \left\{ I_0 - I_4 + 2e\ (2I_1 - I_3 - I_5)\right\} \sin 2\omega$$

$$+ \frac{1}{4} c^2 \left\{ I_1 + \frac{1}{2} e\ (3I_0 + I_2) + \frac{1}{2} FA \left[I_0 + I_2 + e\ (3I_1 + I_3)\right]\right\}$$

$$+ \frac{1}{8} c^2 \left\{ I_3 + I_5 - \frac{1}{2} e\ (3I_1 - 6I_4 - 5I_6) + \frac{1}{2} FA \left[I_2 + 2I_4 + I_6\right.\right.$$

$$\left.\left. + e\ (3I_1 + 5I_3 + I_5 + 3I_7)\right]\right\} \cos 4\omega - \frac{1}{16} c^2\ FB \left\{ I_2 - I_6\right.$$

$$\left. + e\ (3I_1 - 3I_3 - I_5 + 3I_7)\right\} \sin 4\omega \Big\} \quad . \tag{2.10}$$

In the expressions above g is the gravitational acceleration at the surface of the Earth, β is the reciprocal of the density scale height H, and

$$\delta = \left(\frac{C_D S}{W}\right) \left[1 - \frac{r_p}{v_p} \Lambda\omega_e \cos i \right]^2 \quad , \tag{2.11}$$

$$\rho_o = \frac{1}{2} \; (\rho_{max} + \rho_{min}) \quad , \tag{2.12}$$

$$F = \frac{\rho_{max} - \rho_{min}}{\rho_{max} + \rho_{min}} \quad , \tag{2.13}$$

$$A = \sin \delta_B \sin i \sin \omega + \cos \delta_B \left[\cos (\Omega - \alpha_B) \cos \omega - \cos i \sin (\Omega - \alpha_B) \sin \omega\right], \tag{2.14}$$

$$B = \sin \delta_B \sin i \cos \omega - \cos \delta_B \left[\cos (\Omega - \alpha_B) \sin \omega + \cos i \sin (\Omega - \alpha_B) \cos \omega\right], \tag{2.15}$$

$$c = \frac{1}{2} \; \beta r_p \, \epsilon \sin^2 i \quad , \tag{2.16}$$

and the I_n (n = 0, 1, 2, .., 7) are Bessel functions of the first kind and imaginary argument given by:

$$I_n(\beta ae) = \frac{1}{2\pi} \int_0^{2\pi} \cos (nE) \exp\left[\beta ae \cos E\right] dE \quad . \tag{2.17}$$

In equations (2.11) - (2.16) $\frac{C_D S}{W}$ is the inverse ballistic coefficient for the satellite; r_p and v_p are the perigeal radius and velocity; Λ is the ratio of atmospheric rotation rate to Earth rotation rate, ω_e; ρ_{max} and ρ_{min} are the densities at the diurnal bulge location and diametrically opposite the bulge, respectively, at distance r_p; α_B and δ_B are the right ascension and declination of the *diurnal bulge; and ϵ is the ellipticity of the Earth. When using these expressions in the* MEP algorithm of equations (2.1) mean orbital elements and an osculating perigee radius, r_{posc}, are used in their evaluation. The osculating perigee radius is given by

$$r_{posc} = a_m \; (1 - e_m) + r_{sp} \; (f = o) \quad , \tag{2.18}$$

where r_{sp} is defined in the following section. Values for ρ and β are obtained using the NSWC/ Jacchia 1977-Bass model atmosphere.

2.6 First Order Short Periodic Variations

The first order short periodic variations which are used to compute the osculating orbital elements of equations (2.4) and the osculating perigee distance of equation (2.18) are given by:[1]

$$
\begin{aligned}
a_{sp} &= J_2 \left(\frac{R^2}{a}\right)\left\{\left(\frac{a}{r}\right)^3 \left[1 - \frac{3}{2}\sin^2 i + \frac{3}{2}\sin^2 i \cos 2(\omega + f)\right]\right. \\
&\quad \left. -\left(1 - \frac{3}{2}\sin^2 i\right)\ (1 - e^2)^{-3/2}\right\}, \\
e_{sp} &= \frac{1}{2} J_2 \left(\frac{R}{p}\right)^2 \left(1 - \frac{3}{2}\sin^2 i\right)\left\{\frac{1}{e}\left[1 + \frac{3}{2}e^2 - (1 - e^2)^{3/2}\right]\right. \\
&\quad \left. + 3\left(1 + \frac{e^2}{4}\right)\cos f + \frac{3}{2} e \cos 2f + \frac{e^2}{4}\cos 3f\right\} \\
&\quad + \frac{3}{8} J_2 \left(\frac{R}{p}\right)^2 \sin^2 i \left[\left(1 + \frac{11}{4}e^2\right)\cos(2\omega + f) + \frac{e^2}{4}\cos(2\omega - f)\right. \\
&\quad + 5e\cos(2\omega + 2f) + \frac{1}{3}\left(7 + \frac{17}{4}e^2\right)\cos(2\omega + 3f) \\
&\quad \left. + \frac{3}{2} e \cos(2\omega + 4f) + \frac{e^2}{4}\cos(2\omega + 5f) + \frac{3}{2} e \cos 2\omega\right], \\
i_{sp} &= \frac{3}{8} J_2 \left(\frac{R}{p}\right)^2 \sin 2i \left[e\cos(2\omega + f) + \cos 2(\omega + f)\right. \\
&\quad \left. + \frac{e}{3}\cos(2\omega + 3f)\right],
\end{aligned}
$$

$$
\left.
\begin{aligned}
\omega_{sp} &= \frac{3}{4} J_2 \left(\frac{R}{p}\right)^2 (4 - 5 \sin^2 i)(f - M + e \sin f) \\
&+ \frac{3}{2} J_2 \left(\frac{R}{p}\right)^2 \left(1 - \frac{3}{2} \sin^2 i\right) \left[\frac{1}{e} \left(1 - \frac{1}{4} e^2\right) \sin f + \frac{1}{2} \sin 2f \right. \\
&\left. + \frac{1}{12} e \sin 3f\right] - \frac{3}{2} J_2 \left(\frac{R}{p}\right)^2 \left\{ \frac{1}{e} \left[\frac{1}{4} \sin^2 i + \frac{e^2}{2} \left(1 - \frac{15}{8} \sin^2 i\right)\right] \right. \\
&\times \sin (2\omega + f) + \frac{e}{16} \sin^2 i \sin (2\omega - f) + \frac{1}{2} \left(1 - \frac{5}{2} \sin^2 i\right) \\
&\times \sin 2 (\omega + f) - \frac{1}{e} \left[\frac{7}{12} \sin^2 i - \frac{e^2}{6} \left(1 - \frac{19}{8} \sin^2 i\right)\right] \\
&\left. \times \sin (2\omega + 3f) - \frac{3}{8} \sin^2 i \sin (2\omega + 4f) - \frac{e}{16} \sin^2 i \sin (2\omega + 5f) \right\} \\
&- \frac{9}{16} J_2 \left(\frac{R}{p}\right)^2 \sin^2 i \sin 2\omega \quad , \\
\Omega_{sp} &= - \frac{3}{2} J_2 \left(\frac{R}{p}\right)^2 \cos i \left[f - M + e \sin f - \frac{e}{2} \sin (2\omega + f) \right. \\
&\left. - \frac{1}{2} \sin 2 (\omega + f) - \frac{e}{6} \sin (2\omega + 3f)\right] \quad , \\
M_{sp} &= - \frac{3}{2} J_2 \left(\frac{R}{p}\right)^2 \frac{\sqrt{1 - e^2}}{e} \left\{ \left(1 - \frac{3}{2} \sin^2 i\right) \left[\left(1 - \frac{1}{4} e^2\right) \sin f \right. \right. \\
&\left. + \frac{e}{2} \sin 2f + \frac{e^2}{12} \sin 3f\right] + \frac{1}{2} \sin^2 i \left[- \frac{1}{2} \left(1 + \frac{5}{4} e^2\right) \sin (2\omega + f) \right. \\
&- \frac{e^2}{8} \sin (2\omega - f) + \frac{7}{6} \left(1 - \frac{e^2}{28}\right) \sin (2\omega + 3f) \\
&\left. \left. + \frac{3}{4} e \sin (2\omega + 4f) + \frac{e^2}{8} \sin (2\omega + 5f)\right] \right\} \\
&+ \frac{9}{16} J_2 \left(\frac{R}{p}\right)^2 \sqrt{1 - e^2} \sin^2 i \sin 2\omega \quad ,
\end{aligned}
\right\} \quad (2.19)
$$

and

$$r_{sp} = -\frac{1}{2} J_2 \left(\frac{R^2}{p}\right)\left(1 - \frac{3}{2}\sin^2 i\right)\left[1 + \frac{e}{1+\sqrt{1-e^2}}\cos f + \frac{2}{\sqrt{1-e^2}}\left(\frac{r}{a}\right)\right] + \frac{1}{4} J_2 \left(\frac{R^2}{p}\right)\sin^2 i \cos(2\omega + 2f) \quad ,$$

where f is the satellite true anomaly which can be computed from M (see section 4.1). Note that when computing the X_{sp} in equations (2.4) and equation (2.18), mean Keplerian elements are used in the right hand sides of equations (2.19).

2.7 Instantaneous Orbit Parameter Changes Due to Impulsive Thrusting

The changes in orbit parameters due to instantaneous velocity changes are modeled from the results obtained from the Lagrange Planetary Equations.[3] Let the instantaneous velocity change due to an impulsive thrust, $\Delta\vec{V}$, be given by

$$\Delta\vec{V} = \Delta V_R \hat{R} + \Delta V_I \hat{I} + \Delta V_C \hat{C} \quad , \tag{2.20}$$

where

$$\hat{C} = \frac{\vec{r} \times \dot{\vec{r}}}{|\vec{r} \times \dot{\vec{r}}|} \quad , \tag{2.21}$$

$$\hat{I} = \frac{\dot{\vec{r}}}{|\dot{\vec{r}}|} \quad , \tag{2.22}$$

and

$$\hat{R} = \hat{I} \times \hat{C} \quad . \tag{2.23}$$

[3] Fitzpatrick, P. M., *Principles of Celestial Mechanics*, Academic Press, Inc., New York, New York, 1970.

Here $\dot{\vec{r}}$ and $\vec{r}$ are the satellite velocity and position vectors. The instantaneous changes in the Keplerian orbital elements and the period resulting from this velocity change are:

$$
\left.
\begin{aligned}
\Delta a_{OA} &= 2a^2\left(\frac{v}{\mu}\right)\Delta V_I \quad , \\
\Delta e_{OA} &= \frac{r \sin f}{av}\,\Delta V_R + 2\left(\frac{\cos f + e}{v}\right)\Delta V_I \quad , \\
\Delta i_{OA} &= \frac{r \cos(\omega + f)}{(\mu p)^{1/2}}\,\Delta V_c \quad , \\
\Delta \Omega_{OA} &= \frac{r \sin(\omega + f)}{(\mu p)^{1/2} \sin i}\,\Delta V_c \quad , \\
\Delta \omega_{OA} &= -\frac{(1 + e^2)\cos f + 2e}{e\,(1 + e \cos f)\,v}\,\Delta V_R + 2\,\frac{\sin f}{ev}\,\Delta V_I \\
&\quad - \frac{r \sin(\omega + f)\cos i}{(\mu p)^{1/2} \sin i}\,\Delta V_C \quad , \\
\Delta M_{OA} &= n - \left[\frac{1}{a\,(1 - e^2)^{1/2}\,v}\right]\left\{2 \sin f\left[\frac{a\,(1 - e^2)}{e} + re\right]\Delta V_I \right. \\
&\quad \left. - \left[\frac{r}{e}\,(1 - e^2)\cos f\right]\Delta V_C\right\} \quad , \\
\text{and} \quad & \\
\Delta \tau_{OA} &= 3\,\tau a\left(\frac{v}{\mu}\right)\Delta V_I \quad ,
\end{aligned}
\right\} \tag{2.24}
$$

where

$$v = \sqrt{\mu\left(\frac{2}{r} - \frac{1}{a}\right)} \quad , \tag{2.25}$$

$$r = \frac{a\,(1 - e^2)}{1 + e \cos f} \quad , \tag{2.26}$$

and f is the true anomaly at t_{OA}. Note that mean elements are used to evaluate the right hand sides of equations (2.24) - (2.26) when they are used in equations (2.1).

3. INITIALIZATION

3.1 Initial Condition Transformations

The initial orbital elements may be input as either (a) mean Keplerian elements, (b) mean Brouwer elements, or (c) osculating Keplerian elements. Since LAMP prediction modes require mean Keplerian elements as initial conditions, input types (b) and (c) must be transformed to element type (a). If type (b) initial conditions are used, they are first transformed to type (c) elements at epoch t_o through application of the Brouwer-Lyddane[4,5] orbit theory using a vanishing prediction interval (this transformation is described in the following section). The type (c) elements are converted to type (a) by iterating upon the transformation

$$X_{mj}^{(k)}(t_o) = X_{oscj}(t_o) - X_{spj}\left(X_{m_1}^{(k-1)}(t_o), \ldots, X_{m_6}^{(k-1)}(t_o)\right), \; (j = 1, 2, \ldots, 6) , \tag{3.1}$$

until the condition

$$| X_{mj}^{(k)}(t_o) - X_{mj}^{(k-1)}(t_o) | < \epsilon_j , \; (j = 1, 2, \ldots, 6) , \tag{3.2}$$

is satisfied for all j. In the above expressions k is the iteration counter; $X_{mj}(t_o)$, $X_{oscj}(t_o)$, and $X_{spj}(t_o)$ represent the mean and osculating values and the short periodic variation of the $j^{\underline{th}}$ element at epoch t_o; and ϵ_j is the convergence tolerance for the $j^{\underline{th}}$ element. To initiate this iterative process, it is assumed that

$$X_{mj}^{(o)}(t_o) = X_{oscj}(t_o) , \; (j = 1, 2 \ldots, 6) . \tag{3.3}$$

3.2 Brouwer-Lyddane Transformation Theory

The Brouwer-Lyddane theory is used in LAMP to transform mean Brouwer elements to osculating Keplerian elements prior to converting them to mean Keplerian elements. The transformation to osculating Keplerian elements is accomplished by using the following relations with a zero time from epoch, t. The input mean Brouwer elements at epoch t_o are a'', e'', i'', M_o'', ω_o'', and Ω_o''. Define:

$$\left.\begin{aligned} t &= \text{time from epoch} \\ n_o &= (\mu/a''^3)^{1/2} \\ \eta &= (1 - e''^2)^{1/2} \end{aligned}\right]$$

---

[4] Brouwer, D., "Solution of the Problem of Artificial Satellite Theory Without Drag," *The Astronomical Journal,* Vol. 64, No. 1274, 1959, pp. 378-397.

[5] Lyddane, R. H., "Small Eccentricities or Inclinations in the Brouwer Theory of Artificial Satellites," *The Astronomical Journal,* Vol. 68, No. 8, 1963, pp. 555-558.

$$
\left.
\begin{aligned}
\theta &= \cos i'' \\
\gamma_2 &= \frac{1}{2} C_{20} a_e^2 / a''^2 \\
\gamma_2' &= \gamma_2 \eta^{-4} \\
\gamma_3' &= - C_{30} a_e^3 a''^{-3} \eta^{-6} \\
\gamma_4' &= - \frac{3}{8} C_{40} a_e^4 a''^{-4} \eta^{-8} \\
\gamma_5' &= - C_{50} a_e^5 a''^{-5} \eta^{-10} \\
\alpha &= 1 - 5\theta^2 \\
\beta &= 1 - 11\theta^2 - 40\theta^4 \ \alpha^{-1} \\
\gamma &= 1 - 3\theta^2 - 8\theta^4 \ \alpha^{-1} \\
\delta &= 1 - 9\theta^2 - 24\theta^4 \ \alpha^{-1} \\
\lambda &= 1 - 5\theta^2 - 16\theta^4 \ \alpha^{-1}
\end{aligned}
\right\} \tag{3.4}
$$

Then the secular terms are computed from:

$$
\begin{aligned}
M'' = n_o t \Big\{ & 1 + \frac{3}{2} \gamma_2' \eta (3\theta^2 - 1) + \frac{3}{32} \gamma_2'^2 \eta \Big[- 15 + 16\eta + 25\eta^2 \\
& + (30 - 96\eta - 90\eta^2) \theta^2 + (105 + 144\eta + 25\eta^2) \theta^4 \Big] \\
& + \frac{15}{16} \gamma_4' \eta e''^2 \Big[3 - 30\theta^2 + 35\theta^4 \Big] \Big\} + M_o'' \quad ,
\end{aligned} \tag{3.5}
$$

$$
\begin{aligned}
\omega'' = n_o t \Big\{ & - \frac{3}{2} \gamma_2' \alpha + \frac{3}{32} \gamma_2'^2 \Big[- 35 + 24\eta + 25\eta^2 + (90 - 192\eta - 126\eta^2)\theta^2 \\
& + (385 + 360\eta + 45\eta^2) \theta^4 \Big] + \frac{5}{16} \gamma_4' \Big[21 - 9\eta^2 + (-270 \\
& + 126\eta^2) \theta^2 + (385 - 189\eta^2) \theta^4 \Big] \Big\} + \omega_o'' \quad ,
\end{aligned} \tag{3.6}
$$

nd

$$
\begin{aligned}
\Omega'' = n_o t \Big\{ & - 3 \gamma_2' \theta + \frac{3}{8} \gamma_2'^2 \Big[(-5 + 12\eta + 9\eta^2) \theta \\
& + (-35 - 36\eta - 5\eta^2) \theta^3 \Big] + \frac{5}{4} \gamma_4' (5 - 3\eta^2) \theta (3 - 7\theta^2) \Big\} + \Omega_o'' \ .
\end{aligned} \tag{3.7}
$$

The long period (dependent upon g'') terms are computed from:

$$\delta_1 e = \frac{35}{96}\frac{\gamma_5'}{\gamma_2'} e''^2 \eta^2 \lambda \sin i'' \sin^3 \omega'' - \frac{1}{12}\frac{e''\eta^2}{\gamma_2'}\left(3\gamma_2'^2 \beta - 10\gamma_4' \gamma\right)\sin^2 \omega''$$

$$- \frac{35}{128}\frac{\gamma_5'}{\gamma_2'} e''^2 \eta^2 \lambda \sin i'' \sin \omega'' + \frac{1}{4}\frac{\eta^2}{\gamma_2'}\left[\gamma_3' \right. \tag{3.8}$$

$$\left. + \frac{5}{16}\gamma_5' (4 + 3e''^2)\delta\right] \sin i'' \sin \omega'' + \frac{e''\eta^2}{24\gamma_2'}\left[3\gamma_2' \beta - 10\gamma_4' \gamma\right] ,$$

$$M' + \omega' = M'' + \omega'' + \frac{1}{2}\left\{\frac{1}{24\gamma_2'}\left[-3\gamma_2'^2\left\{2 + e''^2 - 11(2 + 3e''^2)\theta^2\right.\right.\right.$$

$$\left. - 40(2 + 5e''^2)\theta^4 a^{-1} - 400e''^2 \theta^6 a^{-2}\right\} + 10\gamma_4'\left\{2 + e''^2\right.$$

$$\left.\left. - 3(2 + 3e''^2)\theta^2 - 8(2 + 5e''^2)\theta^4 a^{-1} - 80e''^2 \theta^6 a^{-2}\right\}\right]$$

$$\left. + \frac{\eta^3}{\gamma_2'}\left[\frac{\gamma_2'^2}{4}\beta - \frac{5}{6}\gamma_4'\gamma\right]\right\}\sin 2\omega'' + \left\{\frac{35}{384}\frac{\gamma_5'}{\gamma_2'}\eta^3 e'' \lambda \sin i''\right.$$

$$+ \frac{35}{1152}\frac{\gamma_5'}{\gamma_2'}\left[\lambda\left\{-e''(3 + 2e''^2)\sin i'' + \frac{e''^3\theta^2}{\sin i''}\right\}\right.$$

$$\left.\left. + 2e''^3 \theta^2 \sin i''\left\{5 + 32\theta^2 a^{-1} + 80\theta^4 a^{-2}\right\}\right]\right\}\cos 3\omega'' \tag{3.9}$$

$$+ \left\{-\frac{\gamma_3' e'' \theta^2}{4\gamma_2' \sin i''} + \frac{5}{64}\frac{\gamma_5'}{\gamma_2'}\left[-e''\frac{\theta^2}{\sin i''}(4 + 3e''^2)\right.\right.$$

$$\left. + e'' \sin i''(26 + 9e''^2)\right]\delta - \frac{15}{32}\frac{\gamma_5'}{\gamma_2'} e'' \theta^2 \sin i''(4 + 3e''^2)$$

$$\times (3 + 16\theta^2 a^{-1} + 40\theta^4 a^{-2}) + \frac{1}{4}\frac{\gamma_3'}{\gamma_2'}\sin i''$$

$$\times \left(\frac{e''}{1 + \eta^3}\right)\left[3 - e''^2(3 - e''^2)\right] + \frac{5}{64}\frac{\gamma_5'}{\gamma_2'}\eta^2 \delta$$

$$\left.\times \left[\frac{e''(-32 + 81e''^4)}{4 + 3e''^2 + \eta(4 + 9e''^2)}\right]\sin i''\right\} \cos \omega'' ,$$

and

$$\Omega' = \Omega'' + \frac{35\gamma_5' e''^3 \theta}{144\,\gamma_2'} \left\{ 5\,\lambda \sin^{-1} i'' + \sin i'' \left[5 + 32\theta^2 a^{-1} + 80\theta^4 a^{-2} \right] \right\}$$

$$\times \sin^2 \omega'' \cos \omega'' + \frac{e''^2 \theta}{12\gamma_2'} \left\{ -3\,\gamma_2'^{\,2} \left[11 + 80\theta^2 a^{-1} + 200\theta^4 a^{-2} \right] \right.$$

$$\left. + 10\,\gamma_4' \left[3 + 16\theta^2 a^{-1} + 40\theta^4 a^{-2} \right] \right\} \sin \omega'' \cos \omega'' \tag{3.10}$$

$$+ \left\{ -\frac{35\,\gamma_5'}{576\,\gamma_2'} e''^3 \theta \left[5\,\lambda \sin^{-1} i'' + \sin i'' \left(5 + 32\theta^2 a^{-1} + 80\theta^4 a^{-2}\right) \right] \right.$$

$$+ \frac{e''\theta}{4\gamma_2' \sin i''} \left[\gamma_3' + \frac{5}{16}\gamma_5' (4 + 3e''^2)\,\delta + \frac{15}{8}\gamma_5' (4 + 3e''^2) \right.$$

$$\left. \times (3 + 16\theta^2 a^{-1} + 40\theta^4 a^{-2}) \sin^2 i'' \right\} \cos \omega'' \quad .$$

The short period (dependent upon E', f', M'') are computed from:

$$a = a'' - a'' \frac{\gamma_2}{\eta^3} (3\theta^2 - 1) + \left[\frac{a''\gamma_2}{(1 - e'' \cos E')^3} \right] \left[3\theta^2 - 1 \right.$$

$$\left. + 3 \sin^2 i'' \cos(2\omega'' + 2f') \right] \quad , \tag{3.11}$$

$$e = e'' + \delta_1 e + \frac{\eta^2 \gamma_2}{2} \left\{ \frac{3\theta^2 - 1}{\eta^6} \left[\frac{e''}{1 + \eta^3} \left\{ 3 - e''^2 (3 - e''^2) \right\} \right. \right.$$

$$\left. + \left\{ 3 + e'' \cos f' \cdot (3 + e'' \cos f') \right\} \cos f' \right] + \frac{3(1 - \theta^2)}{\eta^6} \left[e'' \right.$$

$$\left. \left. + \left\{ 3 + e'' \cos f' (3 + e'' \cos f') \right\} \cos f' \right] \cos (2f' + 2\omega'') \right\} \tag{3.12}$$

$$- \frac{\eta^2 \gamma_2'}{2} (1 - \theta^2) \left[3 \cos (2\omega'' + f') + \cos (2\omega'' + 3f') \right] \quad ,$$

$$i = i'' - \frac{e''\theta}{\eta^2 \sin i''} \delta_1 e + e'' \gamma_2' \theta \sin i'' \sin f' \sin (2f' + 2\omega'')$$

$$+ 2e'' \gamma_2' \theta \sin i'' \cdot \cos f' \cos (2f' + 2\omega'') + \frac{3}{2} \gamma_2' \theta \sin i'' \cos (2f' + 3\omega'') \,, \tag{3.13}$$

$$\omega + M = \omega' + M' + \frac{\gamma_2'}{4}\Big\{-6\,a\,(f' - M'' + e''\sin f') + (3 - 5\theta^2)$$
$$\times\Big[3\sin(2f' + 2\omega'') + 3e''\sin(2\omega'' + f') + e''\sin(2\omega'' + 3f')\Big]\Big\}$$
$$+ \frac{e''\eta^2\gamma_2'}{4(1+\eta)}\Big\{2(3\theta^2 - 1)(\sigma + 1)\sin f' + 3(1 - \theta^2)$$
$$\times\Big[(1 - \sigma)\sin(2\omega'' + f') + (\sigma + 1/3)\sin(2\omega'' + 3f')\Big]\Big\} \tag{3.14}$$

$$\Omega = \Omega' + \Big[2e''\gamma_2'\theta\cos f' + \frac{3}{2}\gamma_2'\theta\Big]\sin(2\omega'' + 2f')$$
$$- e''\gamma_2'\theta\sin f'\cos(2f' + 2\omega'') - 3\gamma_2'\theta\,(f' - M'' + e''\sin f') \quad , \tag{3.15}$$

and

$$e\,\delta\,\ell = \frac{1}{2}\frac{e''\eta^3}{\gamma_2'}\Big\{\frac{1}{4}\gamma_2'\beta - \frac{5}{6}\gamma_4'\gamma\Big\}\sin 2\omega'' - \Big\{\frac{1}{4}\frac{\gamma_3'}{\gamma_2'}\eta^3\sin i''$$
$$+ \frac{5}{64}\frac{\gamma_5'}{\gamma_2'}\eta^3\sin i''(4 + 9e'')\,\delta\Big\}\cdot\cos 2\omega''$$
$$+ \frac{35}{384}\frac{\gamma_5'}{\gamma_2'}\eta^3 e''^2\lambda\sin i''\cos 3\omega'' - \frac{1}{4}\gamma_2'\eta^3\Big\{2(3\theta^2 - 1)$$
$$\times(\sigma + 1)\sin f' + 3(1 - \theta^2)(1 - \sigma)\sin(2\omega'' + f')$$
$$+ (\sigma + 1/3)\sin(2\omega'' + 3f')\Big\} \quad , \tag{3.16}$$

where

$$\sigma = \left(\frac{\eta}{1 - e''\cos E'}\right)^2 + \left(\frac{1}{1 - e''\cos E'}\right) \quad , \tag{3.17}$$

the eccentric anomaly E' is obtained from a Newton-Raphson iteration upon the Kepler equation

$$E' - e''\sin E' = M'' \quad , \tag{3.18}$$

and the true anomaly f′ is found from

$$\sin f' = \frac{\eta \sin E'}{1 - e'' \cos E'} \quad ,$$

$$\cos f' = \frac{\cos E' - e''}{1 - e'' \cos E'} \quad . \tag{3.19}$$

The final osculating values for a, i, and Ω are computed from equations (3.11), (3.13), and (3.15), respectively. Equations (3.5), (3.14), (3.12), and (3.16) are used to calculate final osculating values for M, ω, and e from the following relations:

$$A = e \cos M'' - e\,\delta\,\ell \sin M'' \quad , \tag{3.20}$$

$$B = e \sin M'' + e\,\delta\,\ell \cos M'' \quad , \tag{3.21}$$

$$M = \tan^{-1} (B/A) \quad , \tag{3.22}$$

$$\omega = (M + \omega) - M \quad , \tag{3.23}$$

and

$$e = (A^2 + B^2)^{1/2} \quad . \tag{3.24}$$

4. AUXILIARY COMPUTATIONS

4.1 Initialization and OEP Support Computations

The initialization procedure and the osculating element prediction capability utilize equations (2.19) and, thus, require a method of computing the true anomaly from the mean anomaly. Since the eccentricities of interest are small (e.g. $e \lesssim .1$), a truncated expansion of f in terms of M can be used with sufficient accuracy. This expansion is given by:

$$f = M + 2e \sin M + \frac{5}{4} e^2 \sin 2M + \frac{13}{12} e^2 \sin 3M \quad . \tag{4.1}$$

The initial nodal period τ must also be computed during the initialization phase. It is approximated by:

$$\tau = \left[\frac{2\pi}{2\pi + \dot{\omega}'\tau_K}\right] \tau_K \quad , \tag{4.2}$$

where τ is in seconds,

$$\tau_K = 2\pi \left(\frac{a'^3}{\mu}\right)^{1/2} \quad , \tag{4.3}$$

and

$$\dot{\omega}' = 10^{-6} \left[\frac{5 \cos^2 i' - 1}{a'^{7/2} (1 - e'^2)^2} \right] , \quad (a' \text{ in earth radii}). \tag{4.4}$$

In the above expressions, a', i', and e' are a_{osc}, i_{osc}, and e_{osc} at t_N, the time of the first crossing of the ascending node after t_O. t_N is computed using an iterative procedure and the OEP/STP mode of ephemeris generation.

When generating osculating Cartesian components using the OEP capability, the following transformations are used:

$$\vec{r}_{osc} = a_{osc} \underset{\sim}{Q} \begin{pmatrix} \cos E_{osc} - e_{osc} \\ \sqrt{1 - e_{osc}^2} \sin E_{osc} \end{pmatrix} , \tag{4.5}$$

and

$$\dot{\vec{r}}_{osc} = \frac{(\mu a_{osc})^{1/2}}{a_{osc} (1 - e_{osc} \cos E_{osc})} \underset{\sim}{Q} \begin{pmatrix} - \sin E_{osc} \\ \sqrt{1 - e_{osc}^2} \cos E_{osc} \end{pmatrix} , \tag{4.6}$$

where

$$\underset{\sim}{Q} = \begin{pmatrix} \cos \Omega_{osc} \cos \omega_{osc} - \sin \Omega_{osc} \cos i_{osc} \sin \omega_{osc} & - \cos \Omega_{osc} \sin \omega_{osc} - \sin \Omega_{osc} \cos i_{osc} \cos \omega_{osc} \\ \cos \omega_{osc} \sin \Omega_{osc} + \cos \Omega_{osc} \cos i_{osc} \sin \omega_{osc} & \cos \Omega_{osc} \cos i_{osc} \cos \omega_{osc} - \sin \Omega_{osc} \sin \omega_{osc} \\ \sin i_{osc} \sin \omega_{osc} & \sin i_{osc} \cos \omega_{osc} \end{pmatrix} . \tag{4.7}$$

E_{osc} is the osculating eccentric anomaly computed from Kepler's equation:

$$E_{osc} - e_{osc} \sin E_{osc} = M_{osc} \quad . \tag{4.8}$$

4.2 Drag Decay Rate Support Computations

The drag decay computations can model $C_D S$ as either a constant or time varying quantity (note, however, that $C_D S$ has been treated as a constant in the variational equations). The form used in LAMP is:

$$C_D S = (C_D S)_0 + (C_D S)_1 (t - t_0) + (C_D S)_2 \sin(\omega + \gamma_1) \quad , \tag{4.9}$$

where the $(C_D S)_i$ $(i = 0, 1, 2)$ are constant coefficients and γ_1 is a phase factor.

The location of the diurnal bulge at a given time t is computed from:

$$\delta_B = \delta_\Theta \quad , \tag{4.10}$$

and

$$\alpha_B = \alpha_\Theta + \Delta \ , \tag{4.11}$$

where Δ is the bulge lag angle,

$$\delta_\Theta = \sin^{-1} \left\{ \sin \epsilon_\Theta \sin \lambda_\Theta \right\} \ , \ -\epsilon_\Theta \leqslant \delta_\Theta \leqslant \epsilon_\Theta \quad , \tag{4.12}$$

and

$$\alpha_\Theta = \begin{cases} \eta & , \ 0 < \lambda_\Theta < \pi/2 \\ \pi - \eta & , \ \frac{\pi}{2} < \lambda_\Theta < \pi \\ & \\ \pi + \eta & , \ \pi < \lambda_\Theta < \frac{3\pi}{2} \\ 2\pi - \eta & , \ \frac{3\pi}{2} < \lambda_\Theta < 2\pi \end{cases} \quad , \ 0 \leqslant \alpha_\Theta \leqslant 2\pi \ . \tag{4.13}$$

Here ϵ_Θ is the solar obliquity, λ_Θ is the celestial longitude of the sun given by:

$$\lambda_\Theta = \left(\frac{.9863\pi}{180} \right) \Delta t_V \ , \ 0 \leqslant \lambda_\Theta \leqslant 2\pi \quad , \tag{4.14}$$

and

$$\eta = \sin^{-1} \left\{ \tan \delta_{\odot} \cot \epsilon_{\odot} \right\} . \tag{4.15}$$

Δt_V is the time elapsed in days since the last vernal equinox. It should be noted that

$$\alpha_{\odot} = \lambda_{\odot} \text{ for } \lambda_{\odot} = \frac{j}{2} \pi , \quad (j = 0, 1, 2, 3, 4). \tag{4.16}$$

A constant, yet representative, value for β must be used in equations (2.8), (2.10), and (2.17). Following Santora[2], an average scale height H_{AVG} will be used to evaluate β:

$$\beta^{-1} = H_{AVG} = H_O + SA \cos \theta_{AVG} , \tag{4.17}$$

where

$$H_O = \frac{1}{2} \left(H_{MAX} + H_{MIN} \right) , \tag{4.18}$$

$$S = \frac{H_{MAX} - H_{MIN}}{H_{MAX} + H_{MIN}} , \tag{4.19}$$

and

$$\cos \theta_{AVG} = \left(\frac{1}{z^2} \right) \left[Z_1 + \left\{ - Z_1^2 - 2z^2 Z_2 \right\}^{1/2} \right] . \tag{4.20}$$

In the last four equations A is given by equation (2.14); H_{MIN} and H_{MAX} are the scale heights at distance r_{posc} at declination δ_B on the day side of the earth and diametrically opposite this point, respectively; and

$$z = \frac{a_m e_m}{H_p} , \tag{4.21}$$

$$Z_1 = z (z - 1) - FA (1 + FA)^{-1} , \tag{4.22}$$

$$Z_2 = (1 + FA)^{-1} - z (1 - \frac{1}{2} z) - \frac{1}{2} . \tag{4.23}$$

H_p in equation (4.21) is the scale height at perigee. If the quantity in curly braces in equation (4.20) becomes negative, then

$$\cos \theta_{AVG} = O . \tag{4.24}$$

Finally, it is necessary to adjust the average density, ρ_o, so that it fits the density at perigee. The adjusted ρ_o is given by:

$$\rho_o = \rho_p - \frac{1}{2} (\rho_{max} + \rho_{min}) \, FA \quad , \tag{4.25}$$

where ρ_p is the density at perigee.

4.3 Model Atmosphere Peripheral Support Computations

The atmospheric densities and scale heights used in LAMP are computed using the NSWC/ Jacchia 1977-Bass model atmosphere. In order to compute the density and scale height for a given location, certain peripheral computations must be made and the results supplied to the model atmosphere. These data are the time at which the density and scale height are required in modified Julian days, t_{MJD}; the solar location, $\alpha_\odot$ and $\delta_\odot$; the solar obliquity, $\epsilon_\odot$; the satellite location, α_s and δ_s, at t_{MJD}; the geomagnetic latitude of the satellite at t_{MJD}, ϕ'; the satellite altitude at t_{MJD}, h; the solar flux values at t_{MJD}, $F_{10.7}$ and $\bar{F}_{10.7}$; and the geomagnetic index at t_{MJD}, K_p. The solar location computations are discussed in section 4.2. The remaining information is computed as follows:

$$t_{MJD} = 1721044. + 367y - (7y/4) + d + (s/86400.) - 2400001.0 \quad , \tag{4.26}$$

where y is the year, d is the day of the year, and s is the seconds of the day;

$$\delta_s = \sin^{-1} \left[\sin i \sin (\omega + f) \right] \quad ; \tag{4.27}$$

$$\alpha_s = \begin{cases} \Omega - \alpha' & \text{for } -\frac{\pi}{2} < \omega + f \leqslant \frac{\pi}{2} \\ \Omega + \pi + \alpha' & \text{for } \frac{\pi}{2} < \omega + f \leqslant \frac{3\pi}{2} \end{cases} \quad , \tag{4.28}$$

where

$$\alpha' = \sin^{-1} \left[k \tan \delta_s \cot i \right] \quad , \tag{4.29}$$

and

$$k = \begin{cases} +1 & \text{for } i \leqslant \pi/2 \\ -1 & \text{for } i > \pi/2 \end{cases} \quad ; \tag{4.30}$$

$$\phi' = \sin^{-1} \left[.9792 \sin \delta_s + .2028 \cos \delta_s \cos (L_s - 291°) \right] \quad , \tag{4.31}$$

where L_s is the East longitude of the satellite given by

$$L_s = \begin{cases} \alpha_s - \alpha_G & \text{for } \alpha_G \leqslant \alpha_s \\ 2\pi + (\alpha_s - \alpha_G) & \text{for } \alpha_G > \alpha_s \end{cases} , \tag{4.32}$$

$$\alpha_G = \omega_\oplus (t_{MJD} - t\gamma_{MJD}) , \quad 0 \leqslant \alpha_G \leqslant 2\pi , \tag{4.33}$$

and $\omega_\oplus$ is the rotation rate of the earth and $t_{\gamma MJD}$ is a recent transit time of the vernal equinox and the Greenwich meridian in modified Julian days;

$$h = \left[\frac{a_m(1 - e_m^2)}{1 + e_m \cos f_m}\right] + r_{sp} - \frac{a_\oplus}{\left[1 + \left(\frac{e_\oplus^2}{1 - e_\oplus^2}\right)\sin^2 \delta_s\right]^{1/2}} , \tag{4.34}$$

where $a_\oplus$ and $e_\oplus$ are the semi-major axis and eccentricity of the reference ellipsoid;

$$F_{10.7} = (F_{10.7})_0 + (F_{10.7})_1 (t - t_o) + (F_{10.7})_2 \sin\left[\left(\frac{t - t_o}{D_2}\right)\pi + \gamma_2\right] , \tag{4.35}$$

and

$$\bar{F}_{10.7} = (\bar{F}_{10.7})_0 + (\bar{F}_{10.7})_1 (t - t_o) , \tag{4.36}$$

where γ_2 is a phase factor and D_2 is a constant; and

$$K_p = (K_p)_0 + (K_p)_1 (t - t_o) . \tag{4.37}$$

It should be noted that mean or osculating values for i, ω, and f are used above when in the MEP or OEP mode, respectively.

4.4 User Support Computations

Additional parameters are computed in LASP to support mission analysis. These parameters are the osculating perigee and apogee altitudes $h_{p_{osc}}$ and $h_{a_{osc}}$; the descending leg osculating altitude at a given latitude, $h\delta_{s_{osc}}$; the phase angle for a two satellite system, Ψ; the propellant consumed by an orbit adjust, ΔW_{OA}; and the remaining usable propellant, ΔW.

The altitude parameters $h_{p_{osc}}$, $h_{a_{osc}}$, and $h\delta_{s_{osc}}$ are computed using equation (4.34) where δ_s is computed using

$$\delta_s = \sin^{-1}\left[\sin(\omega_m + f_m)\sin i_m\right] , \tag{4.38}$$

and

$$f_m = o , \tag{4.39}$$

for $h_{p_{osc}}$, and

$$f_m = \pi , \tag{4.40}$$

for $h_{a_{osc}}$. When computing $h\delta_{s_{osc}}$, δ_s is known but the associated f_m must be calculated as follows:

$$f_m = \begin{cases} u - \omega_m & , \text{for } \omega_m \leq u \\ 2\pi - (\omega_m - u) & , \text{for } \omega_m > u \end{cases} , \tag{4.41}$$

where

$$u = \pi - \sin^{-1}\left[\frac{\sin\delta_s}{\sin i_m}\right] . \tag{4.42}$$

The phase angle Ψ is a measure of the departure of a two satellite system from being dynamically synchronized such that at the instant one satellite (termed the lead vehicle) crosses its descending node, the other (trailing vehicle) crosses its ascending node. The time evolution of the phase angle is computed only for the LTP mode and is in terms of the nodal period of the lead satellite τ_L. Thus for the $n^{\underline{th}}$ rev from epoch:

$$\Psi_n = \Psi_{n-1} + \Delta\Psi_n , \tag{4.43}$$

where

$$\Delta\Psi_n = 2\pi \left[\left(\frac{1}{\tau_1} - \frac{1}{\tau_2}\right) \tau_L + \frac{1}{2}\left(\frac{\dot{\tau}_2}{\tau_2^2} - \frac{\dot{\tau}_1}{\tau_1^2}\right) \tau_L^2\right]_n \quad , \tag{4.44}$$

and

$$\dot{\tau}_\ell = \frac{3}{2}\left(\frac{\Delta a_{D\ell}}{a_{m\ell}}\right)_n \quad , \ (\ell = 1,2) \quad . \tag{4.45}$$

The subscripts $\ell = 1, 2$ designate the satellite being referenced. The user must select one of these as the lead satellite, as well as supply the initial phase angle Ψ_0.

The propellant expended during the $i^{\underline{th}}$ orbit adjust is computed using the expression:

$$\Delta W_{OA_i} = \left(\frac{W_i}{gI_{sp}}\right)\Delta V \quad , \tag{4.46}$$

where g is the gravitational acceleration at the Earth's surface, I_{sp} is the thruster specific impulse, W_i is the satellite weight at the time of the orbit adjust, and ΔV is the instantaneous velocity change given by

$$\Delta V = \left(\Delta V_R^2 + \Delta V_I^2 + \Delta V_C^2\right)^{1/2} \quad . \tag{4.47}$$

The satellite weight W_i and weight of remaining usable propellant ΔW_i are computed as follows:

$$W_i = W_{i-1} - \Delta W_{OA_i} - \dot{\overline{W}}_{OPS}\,(t_{OA_i} - t_{OA_{i-1}}) \ , \ W_i > O \quad , \tag{4.48}$$

and

$$\Delta W_i = \Delta W_{i-1} - \Delta W_{OA_i} - \dot{\overline{W}}_{OPS}\,(t_{OA_i} - t_{OA_{i-1}}) \ , \ \Delta W_i \geqslant O \quad , \tag{4.49}$$

where t_{OA_j} is the time of the $j^{\underline{th}}$ orbit adjust and $\dot{\overline{W}}_{OPS}$ ($\geqslant O$) is a user supplied average rate at which propellant is used for nonorbit adjust related operational maintenance. W_o and ΔW_o must be supplied by the user.

5. SOFTWARE DESIGN CONSIDERATIONS

5.1 Basic Requirements

The LAMP software is coded in FORTRAN IV in such a manner that the program is self-documenting and modular in structure. LAMP may be exercised in either the batch mode or an interactive mode with the user. LAMP output may be displayed either as plots or tables, or both. The plots can be generated in either the batch mode or an interactive 'real time' mode.

5.2 Basic Computational Flow

Details associated with the operational options, the output options, and the required input data are delineated in Tables 5-1, 5-2 and 5-3, respectively. A high level computational flowchart is presented in Figure 5-1.

Table 5-1. Operational Options

Option	Flag	Values	Definitions
Prediction Type	IPT	0 1	Mean Element Prediction Osculating Element Prediction
Prediction Mode	IPM	0 1	Short Term Prediction Long Term Prediction
OEP Element Type	IET	0 1	Keplerian Cartesian (For IPT = 1 only)
Display Mode	IDM	0 1 2	List Only Plot Only List and Plot
Initial Input Element Type	IIET	0 1 2	Mean Brouwer Elements Mean Keplerian Elements Osculating Keplerian Elements
Atmospheric Drag Modeling	IAD	0 1	Do Not Include Drag Modeling Include Drag Modeling
Orbit Adjust Modeling	IOA	0 1	Do Not Include Orbit Adjust Modeling Include Orbit Adjust Modeling

*These same operational options apply to each satellite in a multiple satellite case.

Table 5-2. Output Options*

IOP Flag Value	Quantities Displayed†	Comments
0	$t\ a\ e\ i\ \Omega\ \omega\ M$ (or $x\ y\ z\ \dot{x}\ \dot{y}\ \dot{z}$) $(C_D S/W)\ \Psi$	Only when IAD = 1
1	t Rev No. $\tau\ h_{p_{osc}}\ h_{a_{osc}}\ h\delta_{s_{osc}}\ \Psi\ (C_D S/W)\ F_{10.7}\ K_p$	Only when IAD = 1
2	$t\ \tau\ \dot{\tau}\ a\ \dot{a}\ e\ \dot{e}\ h_{p_{osc}}\ h_{a_{osc}}$	Only when IAD = 1
3	$t\ \dot{a}\ \dot{e}\ \dot{\tau}\ (C_D S/W)\ F_{10.7}\ K_p\ h_{p_{osc}}$ (or h_{osc} when IPT = 1)	Only when IAD = 1
4	$t\ \langle \dot{e}_G \rangle\ \langle \dot{\bar{i}}_G \rangle\ \langle \dot{\Omega}_G \rangle\ \langle \dot{\omega}_G \rangle\ \langle \dot{M}_G \rangle$	–
5	$t\ a_{sp}\ e_{sp}\ i_{sp}\ \Omega_{sp}\ \omega_{sp}\ M_{sp}$	–
6	$t\ a_\Theta\ \delta_\Theta\ a_B\ \lambda_\Theta\ F_{10.7}\ \bar{F}_{10.7}\ K_p$	Only when IAD = 1
7	$t\ \delta_s\ a_s\ L_s\ \phi'\ h\ F_{10.7}\ \bar{F}_{10.7}\ K_p\ W\ \Delta W$	Only when IAD = 1
8	$t\ \delta_s\ L_s\ h\ \rho\ \frac{\partial \rho}{\partial h}\ H\ F_{10.7}\ \bar{F}_{10.7}\ K_p$	Only when IPT = 1 and IAD = 1
All IOP Values	$t_{OA}\ f_{OA}\ \Delta V_R\ \Delta V_I\ \Delta V_C\ \Delta V\ \Delta W_{OA}\ W\ \Delta W\ \Delta a_{OA}\ \Delta e_{OA}\ \Delta i_{OA}\ \Delta\Omega_{OA}\ \Delta\omega_{OA}\ \Delta M_{OA}\ \Delta\tau_{OA}\ N_{rev_{OA}}$	Only when IOA = 1 and only once at the time of adjust

*These output options apply to each satellite in a multiple satellite case.
†The phase angle Ψ is only displayed (and computed) for a two satellite case and the LTP mode.

Table 5-3. Input Data Definitions

Input Data	Definition	Comments
t_o	Start time and epoch of input elements	–
t_E	End time for predictions	–
$a_o e_o i_o \omega_o \Omega_o M_o$	Initial orbital elements at t_o	Element type must agree with IIET flag
N_{REV_o}	Initial rev number	Needed when IOA=1 or IOP=1
NSAT	Number of satellites	= 1 or 2.
$W_o, \Delta W_o, \dot{\bar{W}}_{ops}$	See section 4.4	–
I_{sp}	Thruster Specific Impulse	–
Ψ_o	Initial phase angle	Required only when NSAT=2 and IAD=1
$(C_D S)_i$	See Eq. (4.9)	Only when IAD=1
Δ	Subsolar bulge lag angle	
Λ	See Eq. (2.11)	
$(F_{10.7})_i$	See Eq. (4.35)	
γ_2, D_2	See Eq. (4.35)	
$(\bar{F}_{10.7})_i$	See Eq. (4.36)	
$(K_p)_i$	See Eq. (4.37)	
t_γ	Time of last vernal equinox	
$t_{\gamma MJD}$	Time of recent transit of vernal equinox and Greenwich median	
$(N_{REV_{OA}})_i$	Rev number for i^{th} orbit adjust	Only when IOA=1; input for each orbit adjust designed between t_o and t_E.
$(f_{OA})_i$	True anomaly of ignition for i^{th} orbit adjust	
$(\Delta V_j)_i$	R, I, C impulse velocity components for i^{th} orbit adjust [see Eqs. (2.20)-(2.23)]	
Δt	Computation granularity [see Egs. (2.1)-(2.2)]	For IPM=0 only

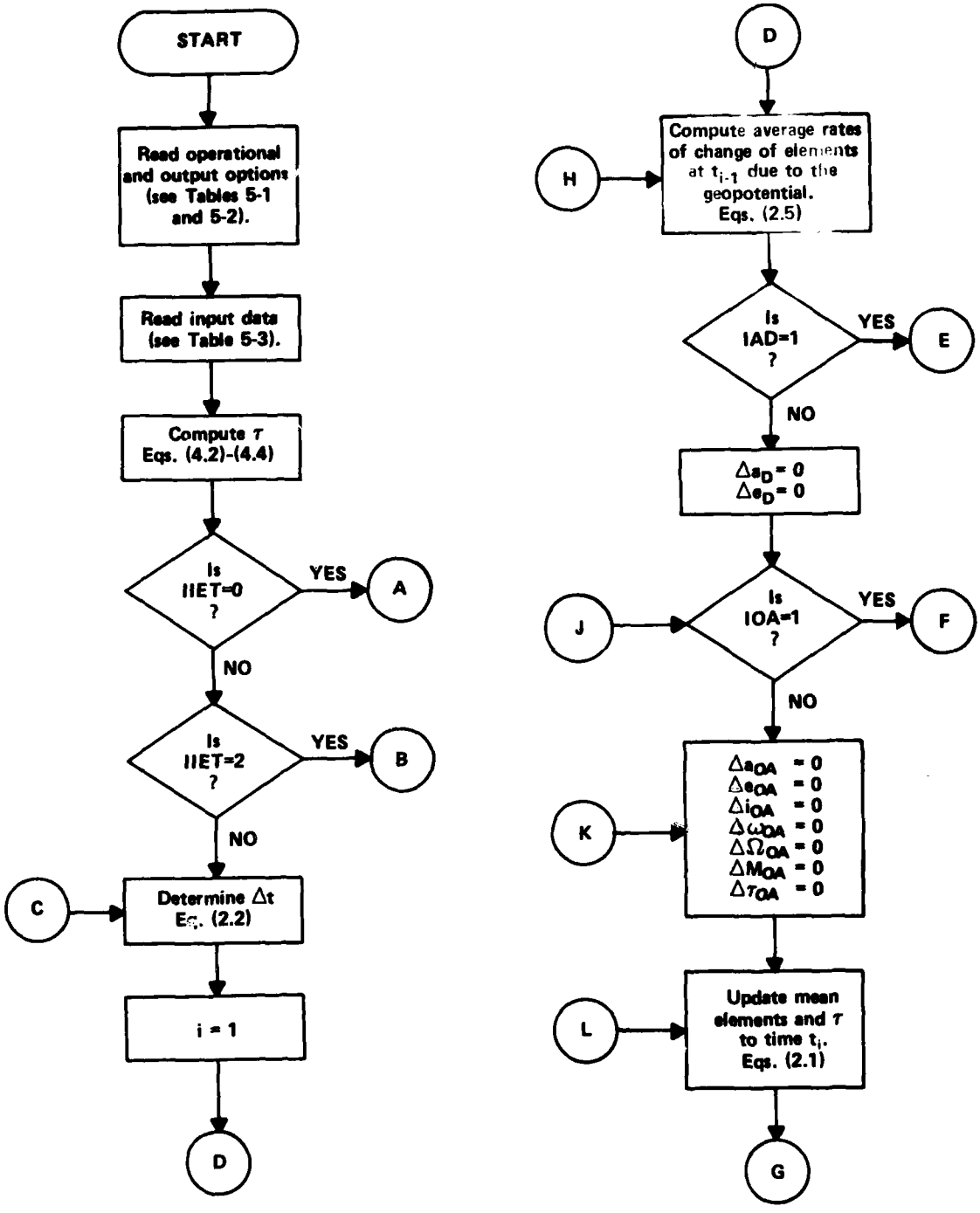

Figure 5-1. LAMP Computational Overview

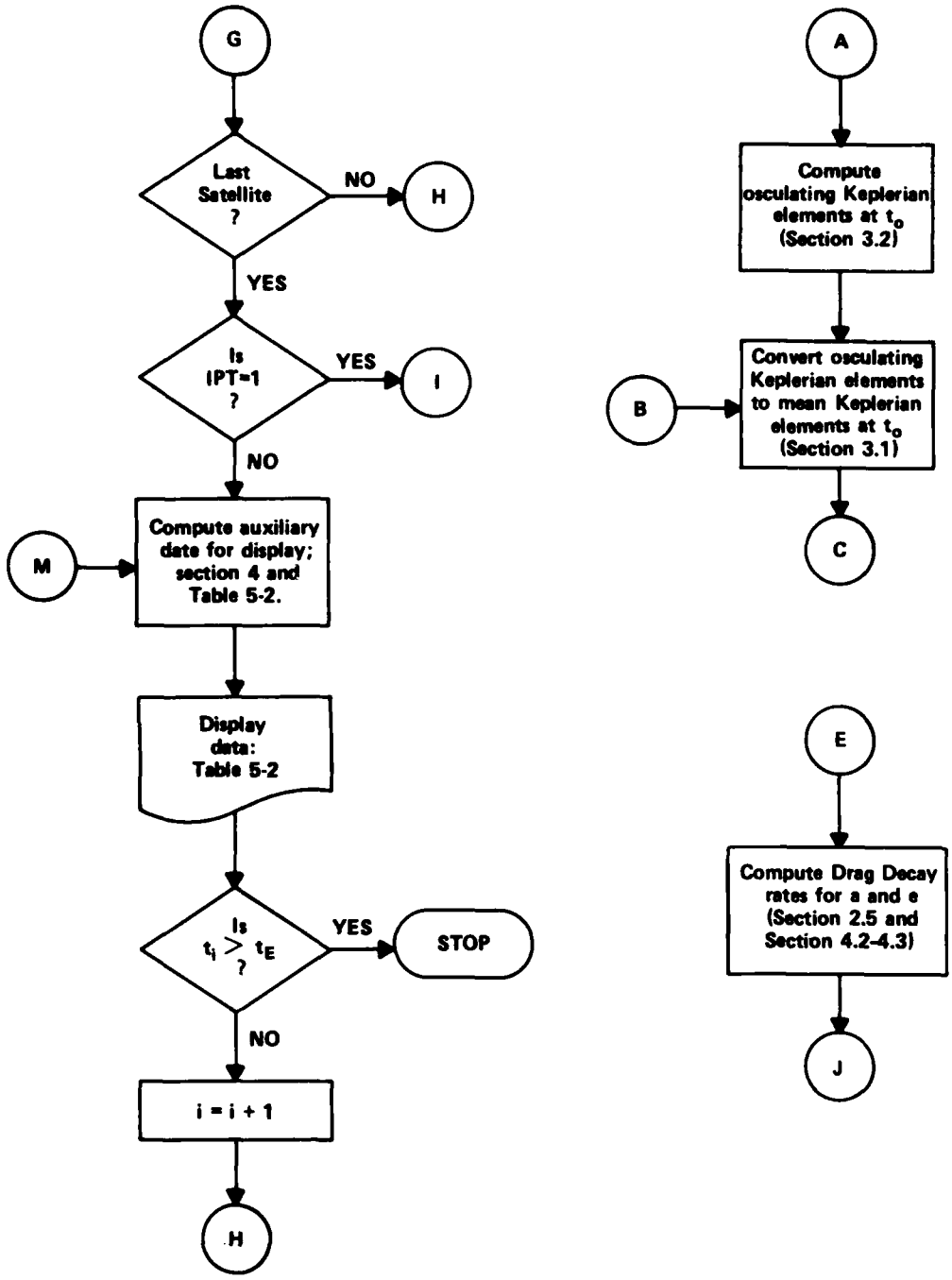

Figure 5-1. LAMP Computational Overview (Continued)

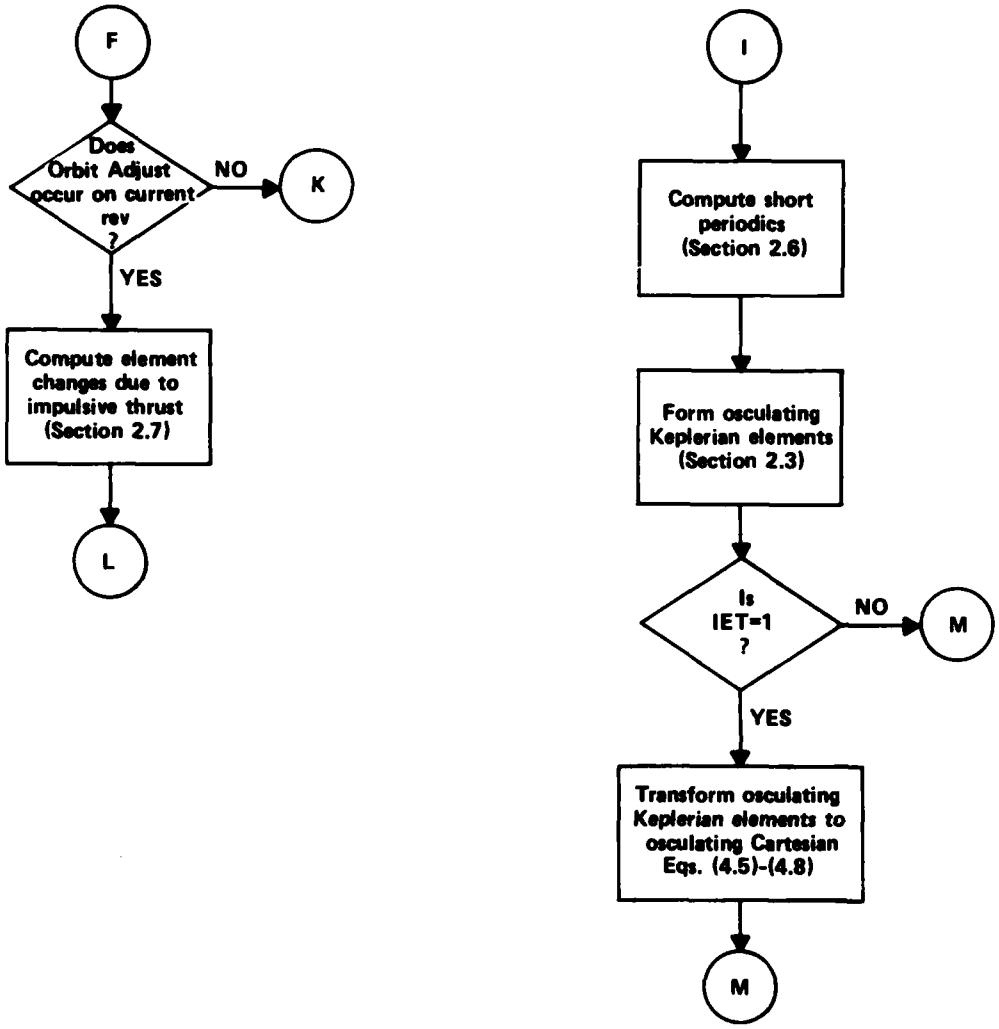

Figure 5-1. LAMP Computational Overview (Continued)

DISTRIBUTION

Defense Technical Information Center Cameron Station Alexandria, VA 22314	(12)
National Aeronautics and Space Administration Scientific and Technical Information Facility Box 5700 ATTN: Technical Library Bethesda, MD 20014	(2)
Defense Mapping Agency Washington, DC 20305	(3)
Defense Mapping Agency Hydrographic/Topographic Center ATTN: Mrs. Caroline Leroy Washington, DC 20390	(6)
Defense Mapping Agency Aerospace Center ATTN: Dr. Robert Ballew St. Louis, MO 63118	(8)
Naval Electronics Systems Command Navy Space Project, PME106 Washington, DC 20360	(3)
Office of Chief of Naval Operations Naval Oceanography Division (NOP-952) Bldg. 1, U.S. Naval Observatory Washington, DC 20390	(2)
Office of Naval Operations Navy Space Systems Division (NOP-943) Washington, DC 20350	(2)
Naval Research Laboratory ATTN: Mr. A. Bartholomew Washington, DC 20375	(3)

Naval Oceanographic Office
Bay St. Louis, MS 39522 (2)

Office of Naval Research
Physical Science Division
800 N. Quincy St.
Arlington, VA 22217 (2)

Air Force Geophysics Laboratory
Hanscom Field
Bedford, MA 01731 (2)
National Oceanic and Atmospheric Administration
National Ocean Survey
ATTN: Dr. John Bossler (3)
Rockville, MD 20850

U.S. Geological Survey
ATTN: Paul Needham (2)
Reston, VA 22091

Goddard Space Flight Center
ATTN: Dr. David Smith (3)
Greenbelt, MD 20771

Jet Propulsion Laboratory
ATTN: Dr. William Melbourne (3)
Pasadena, CA 91103

Applied Research Laboratory
University of Texas
ATTN: Dr. Arnold Tucker (5)
Austin, TX 78712

Local:

E31 (GIDEP)
E411 (Rouse)
K05
K12 (10)
K13 (30)
K14 (5)
X210 (6)